Deformation, Strain, and Pressure-Strain Elastic Modulus at the Supraceliac, Infrarenal, and Mid-Aneurysm Levels in the Aneurysmal Abdominal Aorta

A. S. Les[1], J. J. Yeung[2], G. M. Schultz[2], R. J. Herfkens[3], R. L. Dalman[2], and C. A. Taylor[4]

[1]Bioengineering, Stanford University, Stanford, CA, United States, [2]Department of Vascular Surgery, Stanford University, [3]Radiology, Stanford University,
[4]Bioengineering, Stanford University

Introduction

Abdominal aortic aneurysm (AAA) is the 13th leading cause of death in the United States. As AAAs develop and grow, inflammatory processes weaken and stiffen the aortic wall. Understanding the local strain environment as well as the elastic characteristics of the aortic wall may not only help predict AAA growth and rupture, but is also essential for developing appropriate fixation techniques for aortic stent-grafts, which are typically placed after an aneurysm diameter exceeds 5.5 cm (men) or 4.5 cm (women). While many studies have examined the elastic characteristics of AAAs, few have examined the strain environment and elastic properties of the aorta proximal to an AAA, where aortic stent-grafts are affixed. This study uses a magnetic resonance imaging (MRI) bright-blood technique to quantify luminal strain and elastic properties of the aortic wall at the supraceliac (SC), infrarenal (IR), and mid-aneurysm (MA) locations (Figure 1).

Methods

We imaged 23 men (mean age 66.6±4.7 years) with known small AAAs (<5.0) cm in the supine position using a 1.5T GE MR scanner and an 8-channel cardiac coil. Imaging studies were conducted under a protocol approved by the institutional review board, informed consent was obtained from all subjects, and all patients were screened for contraindications to MR and gadolinium usage, including renal insufficiency. A 3D gadolinium-enhanced magnetic resonance angiography (MRA) sequence was used to image the aorta. A cardiac-gated 2D cine FIESTA sequence (Fast Imaging Employing Steady State Acquisition) was prescribed from the MRA and a localizer scan perpendicular to the aorta at the SC, IR, and MA levels. Luminal motion images were acquired during a single breath-hold (24-45 seconds) and 20 frames were reconstructed over the cardiac cycle. Imaging parameters included a: 224x192 acquisition matrix, 8.0 mm slice thickness, TR of 4.0 ms, TE of 2.0 ms, a 50° flip angle, and 6 views-per-segment. Brachial systolic and diastolic blood pressures were acquired immediately after the scan using an automatic pressure cuff. Of the 23 datasets collected, 9 were excluded from analysis due to poor image quality resulting from failure to complete the breath-hold and/or poor gating for one or more of the luminal motion datasets.

For each patient at each location, the aortic lumen was segmented at each of 20 reconstructed frames using a thresholding technique. The segmentations were smoothed to eight Fourier modes, and the segmental circumference was used to calculate an equivalent diameter. Mean diameter, D_{mean}, and deformation, ΔD ($\Delta D = \text{Diameter}_{max} - \text{Diameter}_{min}$), were calculated. In addition, brachial blood pressures were used to calculate pulse pressure, ΔP ($\Delta P = \text{Pressure}_{systole} - \text{Pressure}_{diastole}$). Brachial blood pressures were assumed to be similar to intraaortic pressure [1]. The circumferential Green-Lagrange strain ($E_{\theta\theta}$), maximum circumferential Green-Lagrange strain (Max $E_{\theta\theta}$), and pressure-strain elastic modulus (E_p) were calculated (equations 1) for each patient at each location.

Results and Discussion

The deformation (ΔD), maximum circumferential Green-Lagrange strain (max $E_{\theta\theta}$), and pressure-strain elastic moduli (E_p) are shown in Table 1. The max $E_{\theta\theta}$ and E_p were not statistically different between the SC and IR locations (p=0.27 and p=0.21, respectively). However, the max $E_{\theta\theta}$ and E_p were statistically significant between the SC and MA locations ($p<0.00001$ and $p<0.0005$) and between the IR and MA locations ($p<0.0005$ and $p<0.0005$). The ΔDs were statistically significantly different between all locations (SC and IR, $p<0.0005$; SC and MA, $p<0.000005$; IR and MA, $p<0.05$). The average E_p at the MA location (2.49 x 10^5 N/m^2) was similar to previously reported values obtained via ultrasound (3.3 x 10^5 N/m^2) [2]. The $E_{\theta\theta}$ at each frame averaged over all 14 subjects are shown in Figure 2. Our work shows that the SC and IR portions of the aorta may experience similar strains, but different deformations. Fixation techniques of aortic stent-grafts may need to account for these different deformations. Additionally, the decreased strain and deformation and increased elastic modulus at the MA location may indicate that thrombus increases the overall stiffness of the aneurysmal wall. It remains to be seen whether patients with decreased MA strain have slower aneurysm growth rates and lower rates of rupture. Future work includes quantifying thrombus burden at the MA location from already-acquired black-blood double-inversion recovery images and exploring the possible correlation between thrombus burden and strain.

$$E_{\theta\theta} = \frac{1}{2}\left(\left(\frac{d_{current}}{D_{\text{minimum}}}\right)^2 - 1\right) \qquad \max E_{\theta\theta} = \frac{1}{2}\left(\left(\frac{D_{\text{maximum}}}{D_{\text{minimum}}}\right)^2 - 1\right) \qquad E_p = \frac{(\Delta P)(D_{mean})}{\Delta D} \qquad (1)$$

Subject	Age	Blood Pressure		Supraceliac (SC)			Infrarenal (IR)			Mid-Aneurysm (MA)		
		Systolic	Diastolic	ΔD (mm)	Max $E_{\theta\theta}$	E_px10^5 N/m^2	ΔD (mm)	Max $E_{\theta\theta}$	E_px10^5 N/m^2	ΔD (mm)	Max $E_{\theta\theta}$	E_px10^5 N/m^2
1	66	149	95	2.07	0.098	0.80	1.26	0.080	0.96	0.97	0.026	2.80
2	61	156	92	2.31	0.097	0.96	1.19	0.072	1.26	1.33	0.050	1.78
3	70	136	80	1.25	0.048	1.62	0.68	0.030	2.52	0.67	0.022	3.43
4	65	144	92	1.56	0.069	1.07	0.91	0.053	1.38	1.18	0.051	1.41
5	73	170	100	1.76	0.067	1.47	1.42	0.079	1.28	0.84	0.027	3.54
6	66	159	103	1.30	0.050	1.55	0.77	0.039	2.00	0.56	0.018	4.17
7	66	119	76	1.57	0.088	0.71	1.19	0.087	0.72	0.97	0.044	1.37
8	62	146	108	1.68	0.083	0.66	1.15	0.068	0.80	0.80	0.026	2.03
9	61	139	91	1.78	0.078	0.89	1.12	0.060	1.12	0.67	0.023	2.82
10	66	124	75	1.69	0.089	0.79	0.78	0.040	1.72	1.22	0.053	1.29
11	69	137	87	1.50	0.058	1.22	1.71	0.092	0.79	0.82	0.035	1.97
12	60	132	78	1.44	0.058	1.31	1.32	0.060	1.26	1.10	0.042	1.77
13	74	125	80	1.08	0.042	1.49	1.26	0.085	0.76	0.56	0.020	3.04
14	73	131	78	2.41	0.110	0.70	1.41	0.085	0.90	0.62	0.021	3.38
Average	**66.6**	**140.5**	**88.2**	**1.67**	**0.074**	**1.09**	**1.15**	**0.066**	**1.25**	**0.88**	**0.033**	**2.49**
Stand. Dev.	**4.7**	**14.4**	**10.7**	**0.38**	**0.021**	**0.35**	**0.29**	**0.020**	**0.52**	**0.25**	**0.013**	**0.94**

Table 1: The age, blood pressures, deformations (ΔD), maximum circumferential Green-Lagrange strains (Max $E_{\theta\theta}$), and the pressure-strain elastic modulus (E_p) for all 14 patients are shown above.

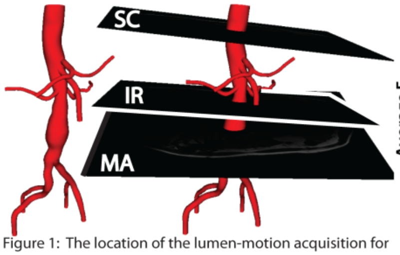

Figure 1: The location of the lumen-motion acquisition for subject 6 is shown above. SC=supraceliac, IR=infrarenal, and MA=mid-aneurysm.

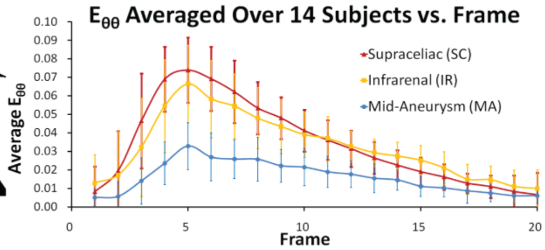

Figure 2: The circumferential Green-Lagrange strains ($E_{\theta\theta}$) at each frame averaged over 14 subjects at the SC, IR, and MA locations are shown above.

References

[1] L. Bax *et al.*, *J Vasc Interv Radiol* **16**, 807 (Jun, 2005).
[2] A. Long *et al.*, *Ann Vasc Surg*, (Oct 28, 2008).